

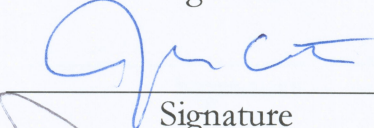
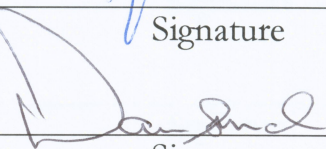


LCLS Engineering Specifications Document #	1.6-111	X-ray End Stations	Revision 0
AMO X-Ray Spectrometers			
John Bozek Author, AMO Scientist			4/17/08 Date
Louis DiMauro AMO Team Leader	SEE ATTACHED PAGE		4/13/08 Date
Stefan Moeller Manager, X-Ray End Stations			4/16/08 Date
John Arthur Manager, Photon Systems			4-18-08 Date
Darren Marsh Quality Assurance Manager			4/15/08 Date

Brief Summary:

The interaction of LCLS FEL x-rays with atomic and molecular samples will create highly excited states that will decay via x-ray emission. X-ray emission provides an additional means (besides electron and ion detection) of investigating the interaction of the FEL pulse with the target atom or molecule. Since photons are detected, rather than charged particles, x-ray emission has the advantage of not being sensitive to charge broadening in the high intensity pulse, and may therefore be better suited to studying higher density samples.

Change History Log

Rev Number	Revision Date	Sections Affected	Description of Change
000	11/23/2007	All	Initial Version

1. Introduction:

Atoms, molecules and clusters irradiated by the intense x-ray beam from the LCLS FEL will potentially undergo multiple excitations and ionizations, resulting in the electronic structure being hollowed out from the inside. If the ionization rate of an inner-shell exceeds the Auger rate, for example, a multiple core hole state could result. The de-excitation dynamics of these highly excited states of matter will be interesting to probe using all of the techniques available including x-ray emission spectroscopy. Additionally, if multiphoton excitation and ionization are efficient in the high field of the focused LCLS x-ray beam, it may be possible to ionize much deeper shells than those accessible with the photon energy available on the soft x-ray branch of the LCLS. A good diagnostic of such multiphoton excitation/ionization would be x-ray emission from the deep inner-shell vacancies. Ar $K\alpha$ and Xe $L\alpha$ radiation, for example, are ~ 3000 and 4000 eV respectively. Observation of these lines would be a clear signature of multiphoton excitation/ionization if the sample were illuminated with 800 - 2000 eV photons. One or more x-ray emission spectrometers imaging the interaction region and dispersing the x-ray spectrum on a shot-by-shot basis are therefore essential tools for the AMO scientific program.

2. Scientific Motivation:

Atoms, molecules and clusters illuminated with high intensity laser radiation are known to form plasmas of highly charged species. X-ray spectroscopy is a principle diagnostic tool of these plasmas since energies of the charged particles are modified by the conditions of the plasma. The high intensity x-ray pulses from the LCLS incident upon atomic, molecular and cluster samples may form previously unobserved states of matter due to the high cross sections for interaction with inner-shell electrons (and corresponding low cross sections for ionization of outer shells). Preliminary results from the FLASH XUV FEL facility in Germany, for example, show that the interaction of intense XUV radiation of 13nm with clusters produces much lower charge states than illumination with longer wavelengths of about 100nm does. Similarly, multiphoton excitation and ionization of deep inner shells of heavy atoms may be better probed with x-ray emission than with photoelectron or Auger electron spectroscopy, since the fluorescence yield increases sharply with Z . Aside from a few studies with light elements, therefore, x-ray energies in the few keV range are most interesting for the AMO experiments.

3. Candidate Spectrometers:

Several types of emission spectrometer could possibly be used for AMO x-ray emission experiments, each with their own strengths and weaknesses.

- 3.1. The first instrument considered was a 5-m spherical grating x-ray emission spectrometer of the Nordgren type (Nordgren and Guo 2000) from Scienta. This high resolution x-ray emission spectrometer is widely in use at many synchrotron radiation facilities. The high dispersion and low efficiency of this spectrometer, however, requires very high sample densities to acquire spectra in reasonable periods of time. Gas cells with thin windows, as are typically used at synchrotrons for gas phase x-ray emission spectroscopy, are not suitable for use with the LCLS beam when it is focused, as the window will not survive the FEL pulse.

- 3.2. Variable line spacing plane grating spectrometers have also been considered, again because of their increasing use at synchrotron radiation facilities. The typical x-ray emission spectrometer designed for use with solid-state physics experiments using synchrotron radiation excitation (Chuang, Pepper et al. 2005), however, is much higher resolution and lower efficiency than that required in the LCLS AMO experiment.

Spectrometers that are used in plasma diagnostics and studies of laser generated plasmas were also considered. Several candidates emerged, depending upon the wavelength regime of interest. Since the lowest photon energy planned to emerge from the undulators in the first phase of the LCLS is 800 eV, spectrometers optimized for photon energies above that value were considered.

- 3.3. The first is a transmission grating spectrometer that has the advantage of very high efficiency and simplicity of design, but suffers from poor resolution (Sailaja, Arora et al. 1998). The high efficiency of the spectrometer, along with the flat detector field, facilitates single shot spectral measurements when used with a position sensitive detector (Sailaja, Arora et al. 2006). The ability to measure an x-ray emission spectrum over a wide range of energies in a single shot is a very appealing capability for early experiments at the LCLS. The energy resolution, typically on the order of 1Å or less, is on the same order as a good energy dispersive analyzer.
- 3.4. The second type of spectrometer considered is a crystal spectrometer operating in the Laue diffraction mode. A similar spectrometer has recently been designed as a diagnostic tool for the National Ignition Facility and utilizes a set of convexly curved crystals to cover the photon energy range from 1 to 23 keV using four different crystals (Hudson, Atkin et al. 2006). Resolving powers of 300-1000 are achieved over the entire range of operation. The spectrometer employs a large area (50 x 25mm) CMOS detector to simultaneously detect a wide range of x-ray energies (E to $\sim 2E$).
- 3.5. Finally, elliptically bent crystal spectrometers of the type described by Henke, with the source at one focus of the ellipse and the spectrum Bragg reflected at normal incidence (Henke, Yamada et al. 1983). This type of spectrometer is also compatible with a position sensitive detector for the simultaneous detection of a large spectral range. Using bent crystals of LiF, PET and KAP photon energies from 500 to 8000 eV can be covered while multilayer reflectors can be used to extend the lower photon energy range down to ~ 100 eV.

To accommodate the needs of the experiment to measure single shot spectra covering a wide energy range, the high resolution grating spectrometers were ruled out as being too specialized for initial experiments. While they will be useful for detailed studies of the electronic states of highly excited matter, this is viewed as a second stage experiment after overviews of the charge states have been determined. The transmission grating spectrometer and elliptically bent crystal spectrometers were selected as the best candidates to provide the wide energy range and single shot capabilities. The convex curved crystal spectrometer is viewed as being more appropriate when higher photon energies need to be detected and will be pursued if very high charge states are accessible with the LCLS beam.

4. Positions of the spectrometers:

X-ray spectrometers can be installed in the 0° and 90° electron spectrometer ports on the high field physics chamber in place of the electron spectrometers when x-ray emission is to be studied. The tightly focused FEL beam will form a well defined source in the dispersive direction of the spectrometers that is extended along the beam direction. If the position of the emission along the length of the beam can be preserved in the spectrometer, i.e. with a two dimensional detector, then x-ray emission can be probed at different power densities as the beam converges to and diverges

from its minimal size in the focus. The length and diameter of the electron TOF spools on the main chamber will determine the focal length of the crystals used in the spectrometers. The x-ray spectrometers could alternatively be mounted on the diagnostics chamber when not in use on the high field physics chamber and operate in a parasitic mode provided clearance is provided in the magnetic shielding for the x-rays to emerge.

5. Transmission Grating Spectrometer:

In the lower energy range of the LCLS beam, a transmission grating spectrometer will be used to measure x-ray emission from atomic, molecular and cluster samples in the AMO instrument. The spectrometer design is extremely simple and can operate over a range from 3 – 90 Å (~100 – 4000 eV) with a resolution of better than 1 Å. The spectrometer is envisioned to use only a free-standing transmission grating in normal incidence followed by a detector with appropriate light baffles to prevent stray radiation from hitting the detector. While better performance can be achieved using grazing incidence imaging optics preceding the grating, they are not compatible with the vacuum environment of the AMO instrument when carrying out studies of materials other than simple atoms. Inclusion of optics in the spectrometer also makes the design and alignment significantly more complex. Additionally, without optics, it is simple to redesign the spectrometer to operate at different source-detector distances, trading off resolution for intensity.

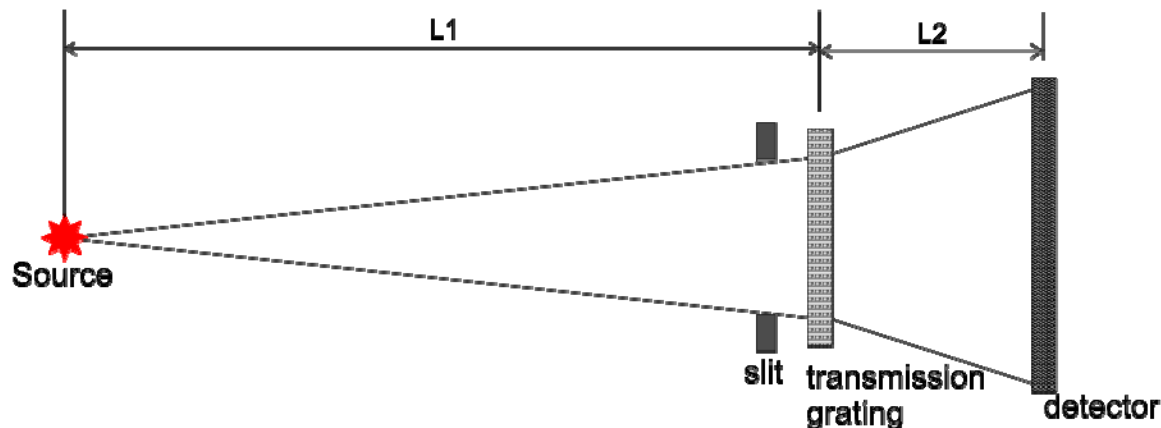


Figure 1: Geometry of a simple transmission grating spectrometer.

A sketch of the simple geometry of the transmission grating spectrometer is shown in the figure above. The total distance from the source to the detector, $D = L_1 + L_2$. The performance of such a simple transmission grating spectrometer is outlined in a 1998 paper by S. Sailaja and parameterized in terms of the distance between the source and the grating and grating and detector as well as the period and illuminated size of the grating. The resolution and signal intensity have conflicting requirements of the source to achieve the best performance, so the distance chosen is necessarily a compromise between signal and resolution as illustrated below. One other contribution to the calculation is the distance from the source to the flange on the electron spectrometer ports, which is 17", and is practically the minimum value for the distance from the source to the grating.

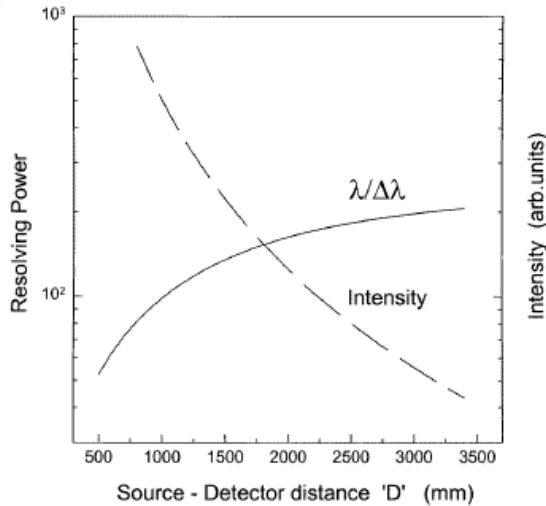


Figure 2: Resolving power and intensity as a function of the distance from the source to the detector (from (Sailaja, Arora et al. 1998)).

Arbitrarily selecting a source to detector distance of 1m, the optimal distance to the grating can be calculated according to:

$$L_1(opt) = \alpha D / (1 + \alpha)$$

$$\alpha = \sqrt{(\Delta S + A) / A}$$

Where ΔS is the source size and A the size of the aperture. Using a conservative source size of 100 μm and an aperture size to match yields an optimal source to grating distance of 586mm (23"), conveniently located beyond the mounting flange so that the entire spectrometer could be mounted in a tube and mounted to the electron TOF flange.

- 5.1. The detector would be located 414mm beyond the grating and would subtend an angles of $\pm 2.77^\circ$, 5.18° and 8.25° for 40mm, 75mm and 120mm detectors respectively, corresponding to maximum wavelengths of 96 \AA (129 eV), 180 \AA (69 eV), and 287 \AA (43 eV) respectively using a 5000 lines mm^{-1} grating.
- 5.2. A multichannel plate intensified phosphor screen detector can be used with this spectrometer to facilitate single-shot spectral measurements. X-rays incident on the MCP surface produce flashes of light on the phosphor screen anode which can then be monitored with a video camera at the pulse rate of the LCLS.
- 5.3. The data is expected to be fairly sparse, given the small solid angle of the spectrometer, so significant data reduction can be carried out in the data acquisition system.
- 5.4. The resolution of the system is calculated to be ~ 70 at 80 \AA , although further optimization is probably possible.
- 5.5. Design considerations:
 - 5.5.1. The design of the spectrometer should include light baffles inserted into the electron TOF spectrometer tube, between the source and the grating, to reduce scattered light.
 - 5.5.2. The width of the aperture in front of the grating should be adjustable with 10 micron reproducibility.
 - 5.5.3. The grating position should be adjustable in the dispersion direction (perpendicular to the FEL beam propagation direction) with 1 μm steps.
 - 5.5.4. The grating should be mounted on a plate that prevents light from passing around the grating but that allows good pumping conductance.

- 5.5.5. A turbo pump should be mounted on the chamber close to the detector.
- 5.5.6. The detector can be mounted on the back flange of the spectrometer vacuum chamber, although care must be taken to ensure that the distance between the grating and detector is constant.
- 5.5.7. Ideally the vacuum chamber should be made of two parts, one that holds the grating and aperture and sets the distance of the grating to the source, and a second that holds the detector and sets the grating to detector distance. This arrangement will make it easy to change the distance between the source and detector to improve the resolution if necessary.

6. Bent Crystal X-ray spectrometer:

Fixed elliptically bent crystal spectrometers have been used successfully by several groups to study laser-produced and discharge type plasmas to identify the charge state of the ions. The source is located in one focus of the crystal's ellipse with the detector located beyond the cross-over point of the second focus. A large range of wavelengths (Bragg angles) can be dispersed onto the detector at time, providing the opportunity to measure energy dispersed spectra on a shot-by-shot basis. In a comprehensive description of the spectrometer geometry, Henke et al. demonstrated that such a spectrometer could be used over a range from 80 – 8000 eV with the appropriate crystal. Each crystal typically covers a photon energy range from E to 2E over diffractions angles of 45° to 135° with E depending on the lattice spacing of the crystal according to the Bragg diffraction equation $n\lambda = 2d \sin \theta$.

Crystal	d (Å)	Energy range for $45^\circ \leq 2\theta \leq 135^\circ$ (eV)	
KAP	26.64	1216	504
PET	8.742	3706	1535
LiF	4.027	8045	4354

The layout of the key parts of the spectrometer is shown below in Figure 3.

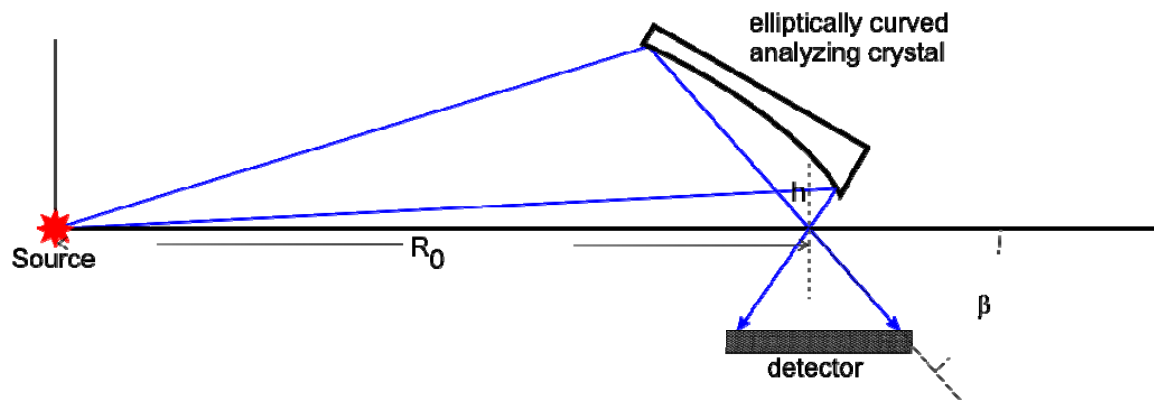


Figure 3: Layout of the elliptically bent crystal x-ray spectrometer.

The shape of the elliptical crystal surface will depend on the distance from the source (R_0) and displacement of the crystal above the focus (h). In the LCLS AMO chamber, the minimum value of R_0 is given by the length of the electron time-of-flight spectrometer tube plus the length of the crystal and/or detector along the same direction. Using a maximal value of 4" for the crystal plus

the 17" from the interaction region to the flange face yields a minimum distance of 21" or 533mm. To provide additional space for mechanical mounting hardware a value of 600mm will be used in the calculations below.

The shape of the elliptical crystal is defined by some simple equations:

$$\rho = \frac{h}{1 - \varepsilon \cos \beta}$$

$$\varepsilon = \sqrt{1 + \left(\frac{h}{R_0}\right)^2} - \frac{h}{R_0}$$

Where ρ is the distance from the cross over point (focus) to the surface, ε is the eccentricity of the ellipse, h is the distance from the central ray on the crystal to the cross over point (ellipse focus), and R_0 is the distance between the foci (source to the cross over point) as defined above in Figure 3 (Henke, Yamada et al. 1983). Solving the above equations for a source distance of 600 mm and a crystal to focus distance of 25mm yields the crystal elliptical surface shown in Figure 4. The 40 mm diameter detector is located about 28mm from the focal point center on a ray extending from the central ray at an angle of 78.5°. The active portion of the crystal surface extends about 30 mm above the central axis (the dashed line extending from the source to the crystal surface in Figure 4). The electron TOF spectrometer nipples on the high field physics chamber have a 4" inner diameter so easily accommodate the required clear aperture.

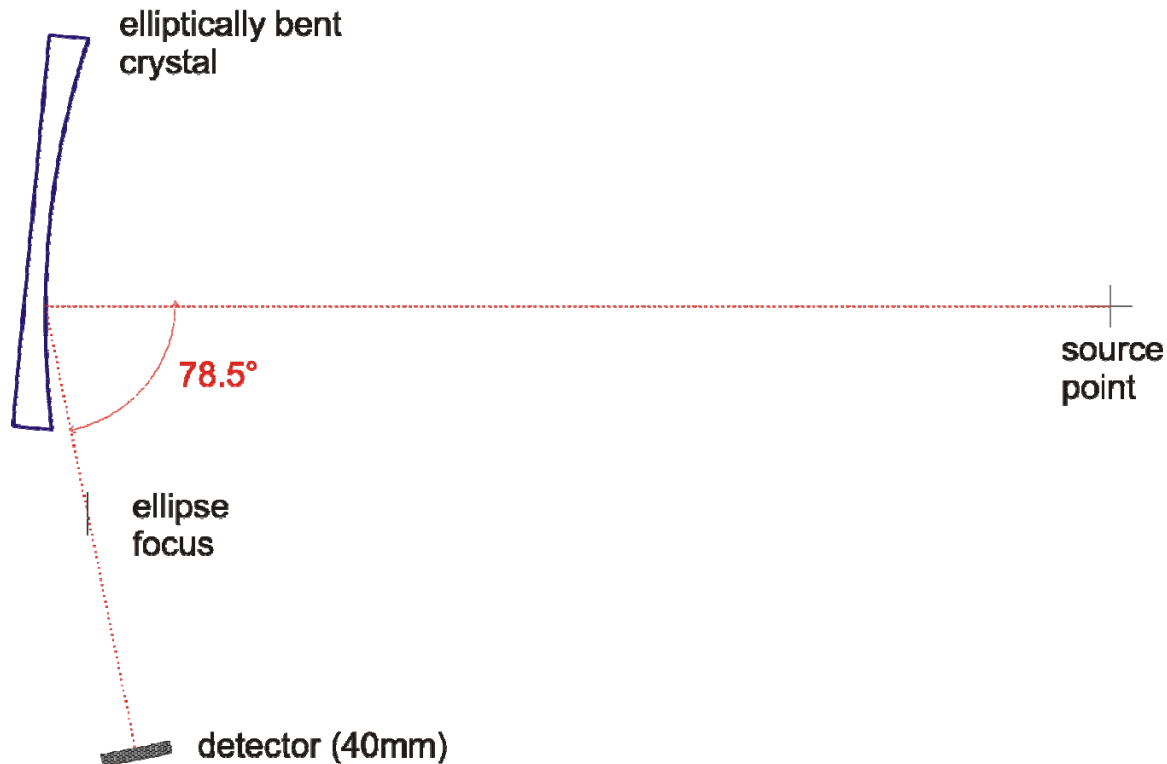


Figure 4: Scaled diagram of the crystal spectrometer (compressed horizontal scale).

7. Controls:

7.1. Both spectrometers are fixed angle instruments and angle scanning is therefore not required.

- 7.2. The transmission grating spectrometer will use an adjustable aperture that must be controlled, along with the position of the grating along a linear slide, however.
- 7.3. Both spectrometers will use MCP enhanced phosphor screen detectors, so high voltages for the detectors will need to be set, controlled and interlocked to the vacuum system.
- 7.4. Each spectrometer will incorporate a turbomolecular pump close to the detector. The pump can be backed by the main chamber vacuum, as is done with the electron TOF spectrometers.

8. Data Acquisition:

Data acquisition will be accomplished by reading the CCD camera imaging the MCP intensified phosphor screen. The camera should be read at the shot rate of the LCLS and the image reduced to a line scan along the dispersive direction. Occasionally it will be advantageous to store the full image, particularly in the beginning when data reduction algorithms need to be developed.

9. References:

- Chuang, Y. D., J. Pepper, et al. (2005). "High-resolution soft X-ray emission spectrograph at advanced light source." Journal of Physics and Chemistry of Solids **66**(12): 2173-2178.
- Henke, B. L., H. T. Yamada, et al. (1983). "Pulsed Plasma Source Spectrometry in the 80-8000-Ev X-Ray Region." Review of Scientific Instruments **54**(10): 1311-1330.
- Hudson, L. T., R. Atkin, et al. (2006). "X-ray spectroscopy at next-generation inertial confinement fusion sources: Anticipating needs and challenges." Radiation Physics and Chemistry **75**(11): 1784-1798.
- Nordgren, J. and J. H. Guo (2000). "Instrumentation for soft X-ray emission spectroscopy." Journal of Electron Spectroscopy and Related Phenomena **110**(1-3): 1-13.
- Sailaja, S., V. Arora, et al. (2006). "Transmission grating spectrograph with on-line recording of XUV soft X-ray spectra from laser produced plasmas." Optics and Laser Technology **38**(1): 46-50.
- Sailaja, S., V. Arora, et al. (1998). "Study of diffraction efficiency of a free-standing transmission grating in keV spectral region using laser produced plasmas." Optics and Laser Technology **30**(6-7): 407-410.